J Solid State Electrochem (2007) 11:1471–1479
DOI 10.1007/s10008-007-0303-7

ORIGINAL PAPER

Charge compensation dynamics in a soluble copolymer of poly(aniline) and poly(phenylene sulfide)

F. F. C. Bazito · S. I. Córdoba de Torresi · R. M. Torresi

Received: 7 February 2007 / Revised: 26 February 2007 / Accepted: 28 February 2007 / Published online: 28 March 2007

Abstract Poly(phenylene sulfide phenyleneamine), PPSA, is a copolymer of poly(aniline) and poly(phenylene sulfide), soluble in conventional organic solvents as tetrahydrofuran, dimethyl sulfoxide, dimethylformamide, and cyclohexanone. In this research, its electrochemical behavior has been studied in acetonitrile in the presence of different electrolytes, where the loss of electroactivity was observed after few cycles. In this paper, the charge compensation dynamics of PPSA is analyzed through electrochemical quartz crystal microbalance experiments and electroacoustic impedance measurements. Raman spectroscopy data have shown that once the oxidation of the sulfur atom occurs, a loss of electroactivity is observed, being not possible to recover the pristine state of the polymer. Fourier transform infrared (FTIR) and X-ray diffraction (XRD) data obtained for the fully oxidized polymer are consistent with the formation of a networked polymer due to the electrophilic attack of the positive sulfur atom on the activated aromatic rings. Electrochemical quartz crystal microbalance results clearly show that the degree of irreversibility fully depends on the chemical nature of the anions with a negligible participation of the cations of the electrolytic solution.

This work is in memoriam of Prof. Dr. Francisco C. Nart, dearest friend and colleague, whose scientific skills and enthusiasm will always be remembered.

F. F. C. Bazito · S. I. Córdoba de Torresi · R. M. Torresi (✉)
Instituto de Química, Universidade de São Paulo,
C.P. 26077, 05513-970 São Paulo, SP, Brazil
e-mail: rtorresi@iq.usp.br

Present address:
F. F. C. Bazito
Universidade Federal de São Paulo, Campus de Diadema,
Diadema, SP, Brazil

Keywords PPSA · EQCM · Charge compensation · Copolymers · Raman

Introduction

In the past few years, the research in electroactive polymers have received considerable attention [1, 2], particularly, aromatic polymers. Among these polymers, poly(aniline) (PANI) has been one of the most widely studied because of its optical and electrochemical properties and due to its chemical and oxidative stability, which make this material suitable for many applications, including rechargeable batteries, corrosion protection, light-emitting diodes, molecular sensors, electrochromic devices, etc. [3–7]. The main structural characteristics in conductive polymers are the linearity and rigidity of the molecule that make these materials insoluble and infusible and, therefore, of difficult processability. PANI has been defined as an insoluble and infusible material under usual conditions. Therefore, several strategies to induce more solubility and processability have been investigated [8–12]. Improved solubility can be achieved by introducing bulky alkyl substituents into the PANI backbone, but limitations are then imposed on the conductivity of the polymer produced. The conductivity of PANI and the solubility of substituted poly(aniline)s can be achieved by copolymerization. These copolymers of aniline and substituted anilines show improved solvent solubility while maintaining high electrical conductivity that can be readily tailored by varying the composition of the copolymer [13, 14].

Besides substituted anilines, other types of monomers can be polymerized with aniline to obtain electroactive copolymers with good mechanical properties. Poly(phenylene sulfide) (PPS) belongs to the same class of PANI, in the

sense that both polymers have certain mobility in the main chain due to the addition of a heteroatom [15]. This polymer presents high crystallinity, good thermal stability, and mechanical resistance. The preparation of a new copolymer containing phenylene sulfide (the monomer of PPS) and phenylene amine units (the monomer of PANI) distributed alternately results in a material with lower crystallinity than its respective homopolymers and, thereby more soluble in organic solvents such as tetrahydrofuran, dimethyl sulfoxide, dimethylformamide, and cyclohexanone and, therefore, processable. This new copolymer, named poly(phenylenesulfide phenyleamine) (PPSA; Scheme 1), was synthesized for the first time in 1996 [16], and ever since, it has been studied due to its interesting properties, such as mechanical stability and electrical conductivity [17–19].

Electrochemical studies carried out in organic media have shown that PPSA is oxidized in two stages. It was reported in a previous work [20] that the oxidation of PPSA in organic solvents, such as acetonitrile (ACN) and propylene carbonate (PC), is only partially reversible during the first cycle. It was also noted that, during the subsequent scans, the redox processes became more reversible with a continuous decrease of current leading to the total loss of electroactivity after ca. 10 cycles. Based on spectroelectrochemical data also published earlier by our group [21], it was pointed out that, at low potentials, PPSA is oxidized reversibly due to the loss of the electron on the nitrogen atom, affording radical cations. When higher potentials are applied, the sulfur atoms are also oxidized, generating dications. However, from the electrochemical point of view, the loss of electroactivity after some redox cycles is a problem that must be overcome, aiming the application of this material in practical devices [21].

In spite of this substantial interest and several studies of the PPSA, there are still many aspects to be clarified about this material. Electrochemical quartz crystal microbalance (EQCM) can be a very useful tool to simultaneously monitor the mass and charge transport in polymeric films, while electroacoustic impedance (EAI) allows monitoring changes in the resonance frequency of the quartz crystal produced by modifications in the bulk or interfacial properties (i.e., viscoelastic film changes or roughness modifications). So that the combination of EQCM, EAI, and spectroscopic techniques such as Raman and IR allows obtaining more information about this polymeric system. In this paper, we discuss the importance of the chemical nature of anions on the irreversibility of the redox processes of PPSA. To achieve this objective, EQCM and EAI, together with Raman and infrared spectroscopies, were used. Experiments were carried out by using different acetonitrile-based electrolytic solutions to put in evidence the role played by either anions or cations in the charge compensation dynamics.

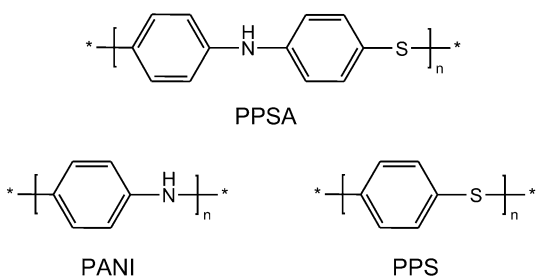

Scheme 1 Structure of poly(phenylenesulfide phenyleneamine) (PPSA)

Experimental

The copolymer PPSA was prepared following the procedure already described in the literature [16, 17] and characterized by spectroscopic techniques. All supporting electrolytes were dried at 80 °C under reduced pressure. The other chemicals were used as received. The solvents used in the reactions and electrochemical experiments were dried by conventional methods and freshly distilled under argon. The electrolytic solutions used were 0.2 mol l^{-1} $LiClO_4$, $LiBF_4$, and NBu_4ClO_4 in acetonitrile.

For the EQCM experiments, the working electrode was a 6 MHz AT cut overtone polished piezoelectric quartz crystal (Valpey–Fisher) with a diameter of 25 mm and a piezo-active electrode area of 0.31 cm^2. Both electrode sides were previously evaporated with gold onto a chromium layer to improve adherence of gold onto the quartz substrate. The polymeric film was deposited on the quartz/Au electrode by casting, using a PPSA solution (2.5 mg in 5.0 ml tetrahydrofolate, THF). It was deposited as three aliquots of 10 μl, consecutively. To assure that all PPSA was deposited onto the piezo-active area, a Teflon o-ring delimiting it was used until complete solvent evaporation. To confirm the amount of PPSA deposited, the quartz resonance frequencies in air before and after deposition were measured, and typically a Δf of 2,700 Hz was obtained, which correspond (using Sauerbrey equation with $K = 6.45 \times 10^7\ Hz\ cm^2\ g^{-1}$) to a mass of 41.9 μg cm^{-2}. Considering that the molar mass of a monomer (Scheme 1) is equal to 200, the amount deposited was 0.21 μmol cm^{-2}. The experiments were carried out in a single compartment electrochemical cell using Pt as the counter electrode. In all experiments, a silver wire was used as quasi-reference electrode. Electrochemical experiments were carried out with a model PG 3901 Omnimetra potentiostat/galvanostat. Frequency shifts during the potential scan were measured by using a Standford Research Systems instrument, model SR620, connected to an

oscillating circuitry (serial mode) and to a microcomputer for data acquisition.

EAI on the modified quartz crystals were carried out to obtain the conductance near the resonant frequency of the crystals. These measurements were made with a HP-4194A frequency impedance meter. The frequency range typically scanned in these experiments was ±30 kHz around the fundamental resonance frequency of 6 MHz. Previous reports have detailed the dependence of the mechanical impedance of quartz crystals on both film and solution properties [22, 23]. By using home-made electrochemical cells and instrumentation, it is possible to make such measurements while one face of the quartz-crystal is in an electrolytic solution and under potential control, allowing the in situ investigation of the mechanical impedance of the PPSA films deposited onto the electrode surface.

Raman spectra were recorded on a Renishaw Raman imaging microscope (System 3000) connected to a CCD detector (Wright, 600×400 pixels), using the 632.8 nm excitation radiation (He–Ne laser, Spectra Physics, model 127).

All baseline corrections were made manually, and all spectra were normalized, using solvent bands as internal reference. In the experiments carried out in acetonitrile, the band at 2,253 cm^{-1} was utilized as reference, which corresponds to the C–N triple bond stretching.

The Fourier transform infrared (FTIR) spectra of pristine PPSA and fully oxidized PPSA as KBr pellets were obtained by using a Bomen MB-100 equipment. X-ray diffractions (XRD) were performed in a Rigaku difractometer by using CuKα radiation source (λ=1.54 Å) in the range from10 to 90°.

Results and discussions

It is well known that EQCM frequency shifts can be influenced by redox-induced changes in the viscoelastic properties of the films being investigated [24]. Thus, before using the simple Sauerbrey relationship to calculate the mass variation from the frequency changes observed during EQCM experiments, it is important to verify that the thin films being studied behave rigidly. Therefore, EAI experiments during electrochemical perturbations were carried out to examine the changes in the mechanical properties of the material during redox cycling [23, 25]. The following experimental protocol was used in these experiments. First, a potential of −0.2 V (reduced state $PPSA_{red}$) was applied for 20 min, allowing the system to reach a steady state. After, this procedure was repeated at 2.0 V (oxidized state $PPSA_{ox}$). EAI data were recorded in the 5.900- and 6.000-MHz frequency range for all the electrolytic solutions studied in this research, $LiClO_4$, $LiBF_4$, and tetrabutylammonium perchlorate (NBu_4ClO_4) in acetonitrile as solvent. Typical conductance spectra, with a maximum at the resonance frequency, were obtained, and the EAI spectra can be analyzed in terms of the full width at half maximum of the conductance peak (Δf_{fwhm}), the maximum of conductance (G_{max}), and the quality factor, which is often a useful measure of the loss of mechanical energy from the vibrating EQCM crystal to the film or solution [24].

The quality factor (Q) can be defined as $Q=f_o/\Delta f_{fwhm}$ (f_o is the frequency of the maximum of conductance). Figure 1 shows the G vs frequency plots for the quartz in the electrolytic solution ACN/$LiCLO_4$; (Fig. 1a) and quartz/PPSA in both redox states, reduced and oxidized (Fig. 1b). For the crystals of the design used in this study, quality factors in air can approach 10^4. The relatively low values observed for the quality factor of the quartz crystal in all these solutions is attributed to the high viscosity of these electrolyte solutions compared with air.

The summary of the results for all solutions are shown in Table 1 for the first cycle. Notable changes in the

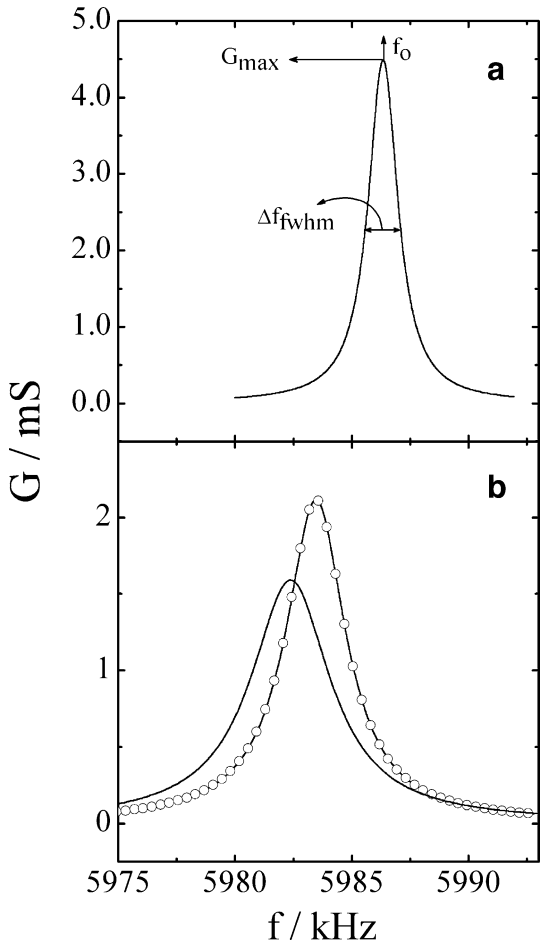

Fig. 1 **a** EIA (conductance) spectrum of quartz electrode and **b** quartz/PPSA electrode at reduced state (−0.2 V, solid line) and oxidized state (2.0 V; *line with circles*). Electrolytic solution, 0.2 mol l^{-1} ACN/$LiClO_4$; frequency sweep, 20 Hz s^{-1}

Table 1 Electroacoustic impedance results for quartz and quartz/PPSA in all electrolyte solutions for the first cycle

Electrolyte	Δf_{fwhm}/Hz			G_{max}/mS			Quality factor		
	Quartz	$PPSA_{red}$	$PPSA_{ox}$	Quartz	$PPSA_{red}$	$PPSA_{ox}$	Quartz	$PPSA_{red}$	$PPSA_{ox}$
$ACN/LiClO_4$	1,500	3,330	4,260	4.4	2.10	1.60	3,985	1,800	1,400
$ACN/LiBF_4$	1,550	3,155	4,505	4.8	2.15	1.25	3,850	1,750	1,420
ACN/Bu_4NClO_4	1,600	3,090	3,985	4.6	2.05	1.63	3,825	1,740	1,380

conductance, full width at half maximum of the conductance peak values, and quality factors were observed from the reduced to the oxidized states for all the electrolytes. Specifically, the decrease in the magnitude of G_{max} (~24%), also in quality factor (~23%), and the increase of Δf_{fwhm} from −0.2 to 2.0 V was observed. The observed differences diminish upon cycling (second cycle onwards) related with the fact that the electroactivity diminishes also with cycling as it will be discussed later. These results show a non-rigid behavior, suggesting that the resonance frequency changes between the two different redox states cannot be attributed only to mass variations. An important modification in the viscoelastic properties and/or surface roughness of the polymer film results in an increase in acoustic energy dissipation within the film when oxidized. For this reason, the Sauerbrey equation [26] ($\Delta f = -K\ \Delta m$) cannot be applied, and all the analyses of quartz crystal microbalance data will be done considering only frequency changes.

Figure 2 shows the j/E and $\Delta f/E$ potentiodynamic profiles obtained with PPSA electrode in a 0.2-mol l^{-1} $ACN/LiClO_4$ electrolytic solution. As it was already reported in previous studies [20, 21], in the first scan (Fig. 2a), only a wide anodic wave with the corresponding cathodic one were observed. The charge associated with the reduction process is significantly smaller than that obtained for the oxidation, indicating that the oxidation of PPSA is only partially reversible. In the subsequent scans, the redox processes become more reversible, considering the higher symmetry between the cathodic and anodic peaks and the charges involved in both processes. The current decreases gradually, and after a few cycles, the film losses its electroactivity.

It is important to note that, depending on the experimental conditions, two peaks are displayed in the first cycle, showing clearly that two electrochemical steps occur in this potential range. Based on the spectroelectrochemical data published earlier by our group [20], it was pointed out that, at low potentials (1.2 V), PPSA is oxidized reversibly due to the loss of the electron on the nitrogen atom, affording radical cations. When higher potentials are applied, the sulfur atoms are also oxidized, generating dications. This latter process is partially reversible, and the sulfur atom was appointed as the main reason for the irreversibility of the PPSA in conventional organic media, according to Scheme 2, probably due to the occurrence of an irreversible chemical reaction.

Considering the total oxidation charge obtained in the first cycle (0.07 C cm^{-2}) and the amount of monomer deposited (0.2 μmol cm^{-2}), it can be calculated that 3.5 e^- are exchanged by each monomeric unit. The reactions described in Scheme 2 show that at least two electrons are exchanged during the full oxidation process so that this result is a clear indication that the film is fully redox converted.

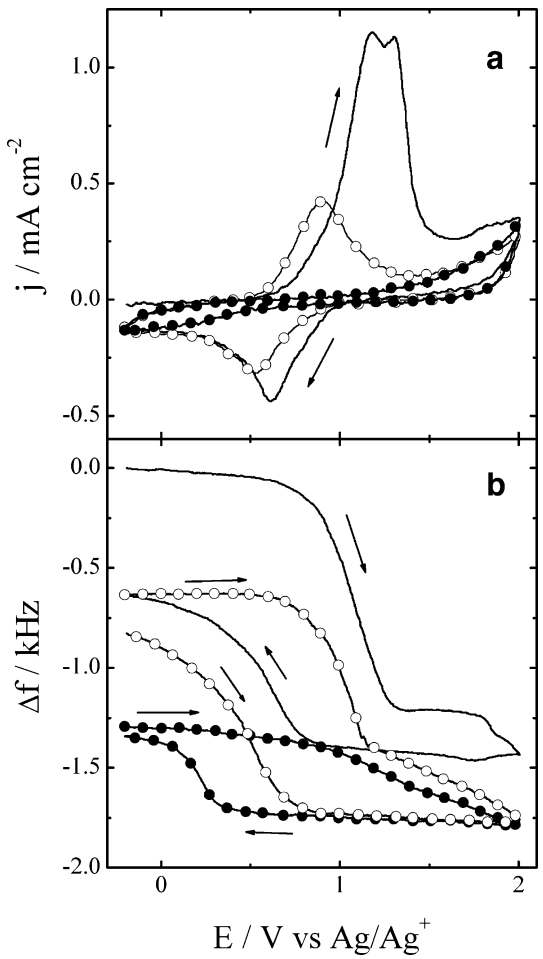

Fig. 2 Potentiodynamic j/E (**a**) and $\Delta f/E$ (**b**) profiles for PPSA films in $ACN/LiClO_4$ electrolytic solution; v=0.01 V/s. *Solid line* first cycle, *line with open circles* second cycle, and *line with full circles* tenth cycle. PPSA deposited mass, 41.9 μg cm^{-2}

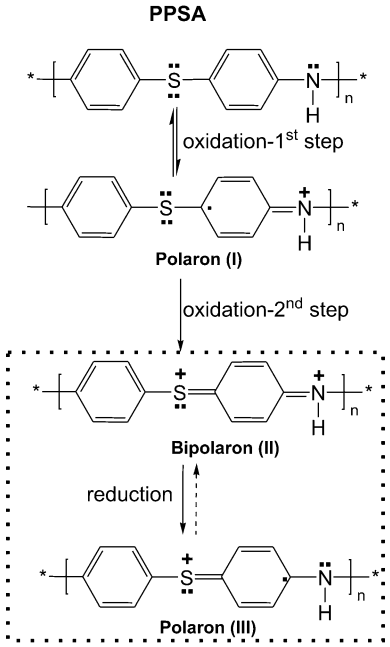

Scheme 2 Complete mechanism for the redox process of the PPSA during the first scan. Inside the *broken-line square* is also represented the second and subsequent scans

Figure 2b shows the $\Delta f/E$ potentiodynamic profile obtained simultaneously with the voltammogram showed in Fig. 2a. During the first cycle, the oxidation process is accompanied by a huge diminution of frequency. Even that, as it was already pointed out, Δf cannot be directly transformed in mass changes; the creation of positive sites in the polymeric backbone should be compensated by the insertion of species (ions plus solvent molecules) in the polymeric matrix. It is worthy to note that, due to the partial reversibility observed during the first cycle, the Δf value after a complete cycle at −0.2 V is much lower than the initial value in the pristine state, indicating that a large amount of species (ions and solvent) would remain inside the film. In analogy to PANI, probably the oxidation of PPSA is accompanied by insertion of anions to maintain the electroneutrality, instead of the expulsion of cations. In turn, when PPSA is reduced, these dopant anions leave the film but not in a reversible way, in the same form that the oxidation charge is not completely recovered during the reduction process. The subsequent cycles where the charge is smaller but the redox process appears to be more reversible, it is still possible to observe the diminution of frequency upon oxidation with the corresponding increase when the film is reduced; however, a diminution of the Δf value can be observed at the final potential of each cycle. This fact can be related to both structural changes (viscoelastic effects) and continuous species uptake. It was reported [20, 21] that the redox process taking place during the subsequent cycles was related to the reaction describe in the broken-line square of Scheme 2. So that, EQCM results should indicate that anions are the main responsible species to maintain electroneutrality during this redox process, but also the loss of electroactivity upon cycling is accompanied by the continuous increase of species trapped inside the polymeric film.

As viscoelastic effects and mass changes can not be separated from EQCM data, aiming to confirm the actual role played by both anions and cations in the redox processes of PPSA, EQCM experiments with different electrolytes were carried out where either the cation or the anion were changed. For the sake of comparison with Fig. 2, maintaining the same anion and changing the cation of the electrolyte, Fig. 3 shows the j/E and $\Delta f/E$ potentiodynamic profiles obtained with a PPSA electrode in a 0.2 mol l^{-1} ACN/NBu_4ClO_4 electrolytic solution. Neither the electrochemical features nor the EQCM results are very different than those observed in Fig. 2 for ACN/$LiClO_4$ solutions.

In this study, the oxidation process also takes place with the simultaneous diminution of frequency. It is also possible

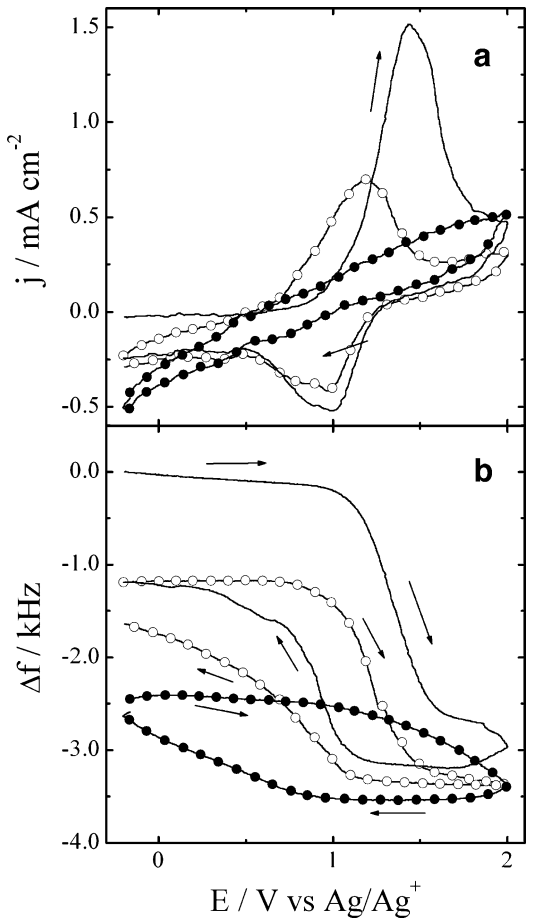

Fig. 3 Potentiodynamic j/E (**a**) and $\Delta f/E$ (**b**) profiles for PPSA films in ACN/Bu_4NClO_4 electrolytic solution; v=0.01 V/s. *Solid line* first cycle, *line with open circles* second cycle, and *line with full circles* tenth cycle. PPSA deposited mass, 43 μg cm^{-2}

to observe that some amount of perchlorate anions must remain inside the film after each cycle, this phenomenon being more evident after the first cycle. It is worth to note at this point that no notable differences were observed by changing the chemical nature of the cation from Li^+ to Bu_4N^+ in spite of the size and the structure of these two cations being so different. This is another indication that the role played by the anions in the ionic exchange is more relevant than that of the other species. To corroborate this statement, experiments were performed in a solution where the chemical nature of the anion was changed. Figure 4 shows the j/E and $\Delta f/E$ potentiodynamic profiles obtained with a PPSA electrode in a 0.2-mol l^{-1} ACN/$LiBF_4$ electrolytic solution.

By comparing with Figs. 2 and 4, it can be seen that the electrochemical behavior of PPSA in this electrolytic solution is completely different. In the first cycle, a very broad voltammetric peak splits in a shoulder at 1.1 V and a maximum at ca. 1.3 V (Fig. 4a) is observed. These processes occur with the concomitant diminution of

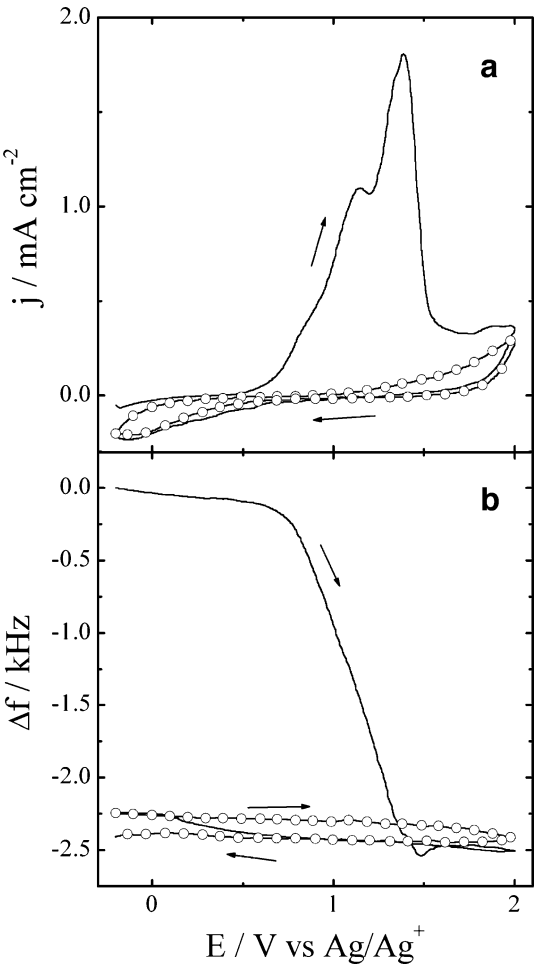

Fig. 4 Potentiodynamic j/E (**a**) and $\Delta f/E$ (**b**) profiles for PPSA films in ACN/$LiBF_4$ electrolytic solution. v=0.01 V/s. *Solid line* first cycle and *line with open circles* second cycle. PPSA deposited mass, 42 μg cm^{-2}

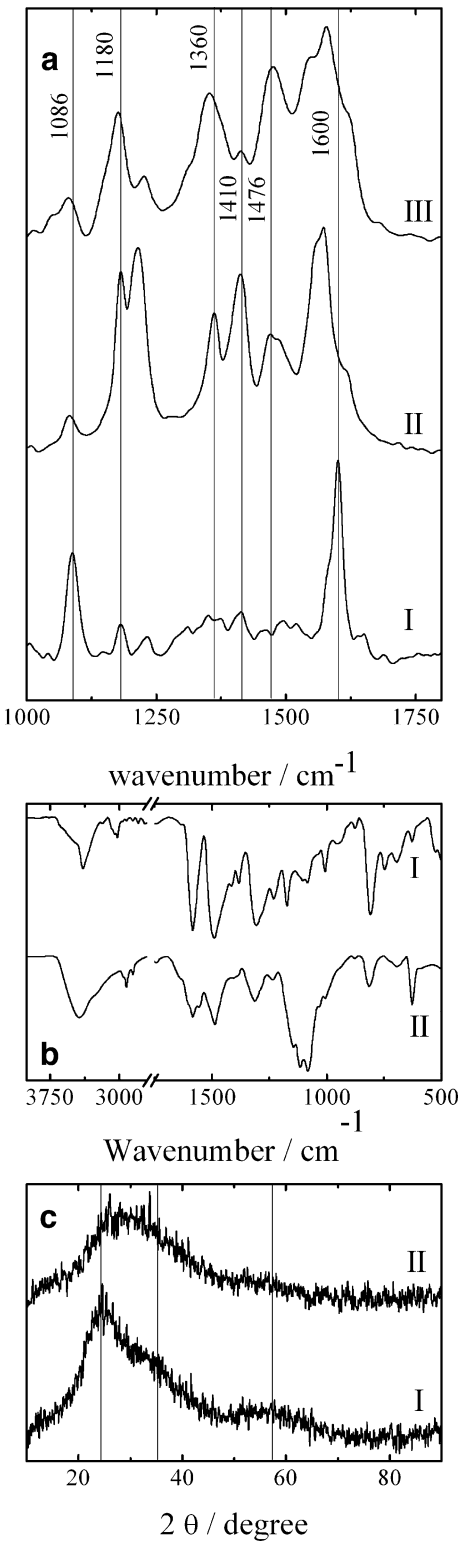

Fig. 5 **a** Raman spectra of a PPSA film recorded at different potentials in ACN/$LiClO_4$ (0.2 mol l^{-1}) electrolyte. Positive going potentials, *I* −0.20 V and *II* 2.00 V. Negative going potentials, *III* −0.20 V; **b** FTIR spectra and **c** XRD pattern of PPSA (*I*) and fully oxidized PPSA (*II*)

frequency (Fig. 4b). When the potential scan is reversed, no reduction peak is observed while the frequency values remain almost constant during the whole cathodic sweep. By analyzing Figs. 2 and 4, the participation of anions in the charge compensation processes was clear so that data shown in Fig. 4 strongly suggest that all the anions inserted during the oxidation process are not ejected during reduction. From the second scan onwards, no electrochemical response is observed in BF_4^- solutions; in the same way, the frequency values do not change. The comparison of this behavior with those obtained in electrolytes based on perchlorate anions will be done later in the light of spectroscopic results.

Raman spectroscopy results obtained simultaneously with electrochemical measurements [20] indicated that, once the oxidation of the sulfur atom takes place, an irreversible chemical reaction occurs. Figure 5a shows "in situ" Raman measurements of PPSA films deposited on Pt electrodes by using excitation line at 632.8 nm in 0.2 mol l^{-1} ACN/$LiClO_4$ recorded at different potentials during the first voltammetric scan. The laser line used was chosen because of resonance effects of charge segments in agreement with electronic spectra data reported before [20]. In this way, bands assigned to oxidized species will be selectively enhanced at this radiation allowing a more detailed analysis.

In the pristine form (Fig. 5a, I), PPSA exhibits four bands. Those at 1,086, 1,230, and 1,600 cm^{-1} are assigned to the C–S, C–N, and C–C aromatic bond stretching vibrations, respectively. In addition, the band at 1,180 cm^{-1} is attributed to the in-plane C–H bending of the aromatic rings. When the polymer is oxidized at 2.0 V (Fig. 5a, II), the spectrum exhibits the decrease of the band at 1,086 cm^{-1}, indicating that the C–S single bond is changing. Due to the oxidation of the sulfur site, dicationic structures (quinoids units) are formed, and this fact is corroborated by the broadening of the band at 1,600 cm^{-1} and the appearance of the bands at 1,121 and 1,360 cm^{-1} associated to the presence of quinoid rings [26–29]. In addition, the band at 1,476 cm^{-1}, characteristic of $C{=}N^+$ stretching, emphasizes the formations of dications.

Once the sulfur heteroatom is oxidized, destroying the single bond character (νC–S around 1,086 cm^{-1}), this site is not reduced, and thereby, this band is not reestablished upon reduction at −0.2 V (Fig. 5a, III); the spectrum recorded at the end of the cycle (Fig. 5a, III) is not identical to the pristine PPSA (Fig. 5a, I). Moreover, the aromatic ring vibration still remains altered, suggesting a modification of the environment around this ring. Although the spectra recorded during the second cycle are not shown in this paper, it is important to mention that the C–S stretching is not reestablished, showing that this site does not participate during the second and subsequent cycles, and the observed changes are only associated with the oxidation/reduction of the C–N bond [20]. The resonant Raman results obtained in ACN/$LiBF_4$ solutions (not shown) also demonstrate that the C–S bond is not recovered after oxidation.

An explanation for the irreversibility of the C–S bond character is that the positive charges sulfur atom formed after its oxidation (see Scheme 1) could act as an electrophile, and then, it would react with other highly activated aromatic rings towards electrophilic aromatic substitution (EAS), leading to the formation of a cross-linked polymeric matrix, according to the simplified Scheme 3. In this case, during a few cycles, the N segments still remains active toward sulfur reduction as shown in Scheme 3.

To elucidate such irreversibility, FTIR spectra (Fig. 5b) and X-ray diffractograms (Fig. 5c) of both pristine PPSA (I) and fully oxidized PPSA (II) in the solid state have been analyzed. It is possible to observe important differences between the FTIR spectra of pristine and oxidized polymer. The downward shift of the N–H stretching (ca. 3,430 cm^{-1}) is probably due to changes of the N–H hydrogen bonding in the oxidized PPSA, due to the intercalation of perchlorate ions. The presence of these ions is also confirmed by the appearance of the band at 1,171 cm^{-1}, in good agreement with EQCM results. Another change is observed in the region of C–H aromatic stretching absorptions (3,100–2,900 cm^{-1}), where the decrease of intensity and the shift of the bands must be related to the formation of aromatic rings with substitution pattern distinct to the original polymer. The bands assigned to C–S stretching (1,103 and 1,081 cm^{-1}) decrease strongly, and those at 1,007 and 501 cm^{-1} can be attributed to the vibrations of units similar to $(Ar)_3S^+$ (Ar=Aryl groups) as it was reported before [30–32]. It is known that bands below 900 cm^{-1} are quite sensitive to changes in the nature, number, and position of substituents in aromatic rings, being extremely

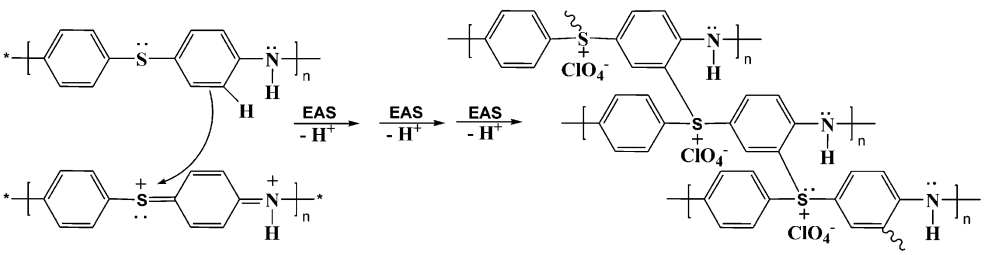

Scheme 3 Schematic representation of the networked polymer formed in the fully oxidized PPSA

useful for determining the substitution pattern [33]. The shift of the band at 815 to 810 cm^{-1}, the appearance of another one with lower intensity (ca. 750 cm^{-1}), and the decrease of the intensity at 628 cm^{-1} suggest the formation of 1,2,4-trisubstituted aromatic rings. This is also corroborated by the band at 1,884 cm^{-1} assigned to the overtones in combination with the bands of the out of plane C–H deformation vibration. Obviously, some 1,4-aromatic rings are conserved but it is clear that some rings change their substitution pattern, in agreement with Scheme 3. In Fig. 5c, II, it can be seen that the oxidized form of PPSA is less crystalline than the pristine material with broad Bragg diffraction peaks at 2θ=25, 33, and 55°. The formation of structures like $(Ar)_3S^+$ represented in Scheme 3 should decrease the linearity of the original polymer, and therefore, they will diminish the crystallinity of the pristine material. The decrease of the number of hydrogen bonds in the oxidized material should be the main reason for this increase of amorphousness. Moreover, the formation of $(Ar)_3S^+$ units in the polymer backbone should block the conjugation along the chain; this fact is corroborated by the loss of electroactivity upon cycling.

This assumption is coherent with the insolubility and infusibility of the resulting fully oxidized polymer, and also, it is in good agreement with EAI results where a huge change in the viscoelastic properties of the film upon oxidation was observed (Table 1). The presence of positive charges in this cross-linked polymer explains the irreversible permanence of perchlorate anions inside the film and the partial reversibility of the first cycle. This statement is also supported, taking into account that the preparation of poly(arylene)sulfides (PAS) by electrophilic substitutions leads predominantly to the cyclization of the chains and to the formation of ladder structures, mainly with the formation of thianthrene type structures [32, 33]. It is also known that diphenyl sulfide in the presence of Lewis acids affords an electrophile (the sulfur atom carries a positive charge) that will react with other monomers to produce PAS [34, 35].

EQCM results clearly indicate that anions are irreversibly inserted during the oxidation of the polymeric film but, while in perchlorate-containing solutions, the complete loss of electroactivity is only achieved after ca. ten cycles; in tetrafluoroborate, no current reduction is observed just after the first anodic scan. That is to say that the reaction presented in Scheme 2 (inside the broken-line square) between polarons (III) and bipolarons (II) takes place only in the presence of ClO_4^-. On the contrary, in BF_4^--containing solutions, the electrophilic reaction occurs in a higher extent till the depletion of the positive sulfur sites, leading to the complete loss of electroactivity. An explanation is due to the higher charge/mass ratio of BF_4^- and also its higher ability to form hydrogen bonds; so, these anions can be easily intercalated and remain tightly bonded to the polymeric matrix. In this way, the kinetics of electrophilic reaction shown in Scheme 3 is more favored than in the presence of perchlorate anions, leading to a faster conversion of all positive sulfur sites into a cross-linked network.

Conclusions

In this work, the charge compensation dynamics of the copolymer PPSA was studied by using EQCM and EAI techniques. The energy dissipation due to the structural modifications of the PPSA matrix was put in evidence by the diminution of the conductance of the quartz crystal when PPSA was oxidized. By this reason, it was not possible to use the Saurbrey equation to transform frequency shifts in mass changes. However, EQCM results have clearly indicated that the redox processes strongly depend on the chemical nature of anions, increasing their irreversibility from perchlorate to tetrafluoroborate anions with no significant influence of cations. This irreversibility was confirmed by using Raman, FTIR, and XRD techniques. The spectra show that the fully oxidized polymer is consistent with the formation of a networked polymer due to the electrophilic attack of the positive sulfur atom on the activated aromatic ring.

Acknowledgment This work was supported by FAPESP (03/10015-3) and CNPq. We also thank the Laboratorio de Espectroscopia Molecular (IQ-USP) for Raman facilities.

References

1. Genies EM, Hany P, Jantier C (1988) J Appl Electrochem 18:751
2. Skotheim TA (1987) Handbook of conducting polymers. Marcel Dekker, New York
3. Anderson MR, Mattes BR, Reiss H, Kaner RB (1991) Science 252:1412
4. Liang WB, Martin CR (1991) Chem Mater 3:390
5. Gustafsson G, Cao Y, Traecy GM, Klavetter F, Colaneri N, Heeger AJ (1992) Nature 357:477
6. Grem G, Leditzky G, Ullrich B, Leising G (1992) Adv Mater 4:36
7. Barlett PN, Birkin PR (1993) Synth Met 61:15
8. Genies EM, Noel P (1991) J Electroanal Chem 31:89
9. Li S, Dong H, Cao Y (1989) Synth Met 29:329
10. Bae WJ, Jo WH, Park YH (2003) Synth Met 132:239
11. Dao LH, Leclerc M, Guay J, Chevalier JW (1989) Synth Met 29:377
12. Park JW, Shin HC, Lee Y, Son Y, Baik DH (1999) Macromolecules 32:4615
13. Wei Y, Hariharan R, Patel S (1990) Macromolecules 23:758
14. Schemid AL, Lira LM, Córdoba de Torresi SI (2002) Electrochim Acta 47:2005
15. Winokur MJ (1997) Handbook of conducting polymers. In: Skotheim TA, Elsenbaumer RL, Reynolds JR (eds). Marcel Dekker, New York, pp 708–725

16. Wang LX, Guth TS, Havinga E, Mullen K (1996) Angew Chem Int Ed 35:1495
17. Leuninger J, Wang C, Guth TS, Enkelmann V, Pakula T, Mullen K (1998) Macromolecules 31:1720
18. Li GF, Josowicz M, Janata J, Mullen K (2001) J Phys Chem B 105:2191
19. Bassler H, Tak YH, Leuninger J, Mullen K (1998) J Phys Chem B 102:4887
20. Bazito FFC, Córdoba de Torresi SI (2006) Polymer 47:1259
21. Bazito FFC, Silveira LT, Torresi RM, Córdoba de Torresi SI (2007) Electrochim Acta (in press). DOI 10.1016/j.electacta.2006.12.055
22. Martin SJ, Granstaff VE, Frye GC (1991) Anal Chem 63:2272
23. Hillman AR (2003) Encyclopedia of electrochemistry, vol. 3. In: Bard AJ, Stratmann M (eds) Wiley, New York, pp 230–289
24. Buttry DA, Ward MD (1992) Chem Rev 92:1355
25. Varela H, Malta M, Torresi RM (2000) Quim Nova 23:664
26. Sauerbrey G (1959) Z Phys 155:206
27. Silva JEP, Faria DLA, Cordoba de Torresi SI, Temperini MLA (2000) Macromolecules 33:3077
28. Silva JEP, Cordoba de Torresi SI, Temperini MLA, Gonçalves D, Oliveira Jr ON (1999) Synth Met 101:691
29. Silva JEP, Temperini MLA, Cordoba de Torresi SI (1999) Electrochim Acta 44:1887
30. Sergeyev VA, Nedelkin VI (1986) J Polym Sci A Polym Chem 24:3153
31. Dektar JL, Hacker NP (1990) J Am Chem Soc 112:6004
32. Miyatake K, Yamamoto K, Endo K, Tsuchida E (1998) J Org Chem 63:7522
33. Imazeki S, Sumino M, Fukasawa K, Ishihara M, Akiyama T (2004) Synthesis 10:1648
34. Piaggio P, Musso GF, Dellepiane G (1995) J Phys Chem 99:4187
35. Yamamoto K, Yoshida S, Nishide H, Tsuchida E (1989) Bull Chem Soc Jpn 62:3655